



Published in final edited form as:

*JACC Basic Transl Sci.* 2017 March ; 2(2): 160–180. doi:10.1016/j.jacbts.2016.12.002.

## A Sarcoplasmic Reticulum Localized Protein Phosphatase Regulates Phospholamban Phosphorylation and Promotes Ischemia Reperfusion Injury in the Heart

Toru Akaike, M.D., Ph.D.<sup>1,2</sup>, Na Du, M.D., Ph.D.<sup>1</sup>, Gang Lu, Ph.D.<sup>1</sup>, Susumu Minamisawa, M.D., Ph.D.<sup>2</sup>, Yibin Wang<sup>\*</sup>,<sup>1</sup>, and Hongmei Ruan, M.D., Ph.D.<sup>\*</sup>,<sup>1</sup>

<sup>1</sup>Department of Anesthesiology and Molecular Biology Institute, University of California, Los Angeles, Los Angeles, CA 90095-1735

<sup>2</sup>Department of Cell Physiology, The Jikei University School of Medicine

### SUMMARY

Phospholamban (PLN) is a key regulator of sarcolemma calcium uptake in cardiomyocyte, its inhibitory activity to SERCA is regulated by phosphorylation. PLN hypophosphorylation is a common molecular feature in failing heart. The current study provided evidence at molecular, cellular and whole heart levels to implicate a sarcolemma membrane targeted protein phosphatase, PP2Ce, as a specific and potent PLN phosphatase. PP2Ce expression was elevated in failing human heart and induced acutely at protein level by  $\beta$ -adrenergic stimulation or oxidative stress in cardiomyocytes. PP2Ce expression in mouse heart blunted  $\beta$ -adrenergic response and exacerbated ischemia/reperfusion injury. Therefore, PP2Ce is a new regulator for cardiac function and pathogenesis.

### Keywords

Phospholamban; Phosphatase; heart

### INTRODUCTION

Heart disease is a leading cause of death in the United States. Defects in intracellular  $\text{Ca}^{2+}$  homeostasis have been implicated in the onset and progression of heart failure (1-6) which lead to blunted response to adrenergic stimulation and loss of contractility (7-9). Cardiac sarcoplasmic reticulum (SR)  $\text{Ca}^{2+}$  cycling, involving  $\text{Ca}^{2+}$  induced  $\text{Ca}^{2+}$  release (CICR) from SR through ryanodine receptor (RyR2) during systole and  $\text{Ca}^{2+}$  uptake via SR calcium-

<sup>\*</sup>Corresponding Authors: Yibin Wang, Ph.D., Cardiovascular Research Laboratories at UCLA, Department of Anesthesiology, Charles E Young Dr. South 650, Los Angeles, CA 90095, Phone:310- 206-4438; Fax:310-206-5907; yibinwang@mednet.ucla.edu OR Hongmei Ruan, M.D., Ph.D., Cardiovascular Research Laboratories at UCLA, Department of Anesthesiology, Charles E Young Dr. South 650, Los Angeles, CA 90095, Phone:310- 206-4438; Fax:310-206-5907; hmruan@ucla.edu.

**Disclosure:** Authors declare no disclosure of any conflicts related to this work.

**Publisher's Disclaimer:** This is a PDF file of an unedited manuscript that has been accepted for publication. As a service to our customers we are providing this early version of the manuscript. The manuscript will undergo copyediting, typesetting, and review of the resulting proof before it is published in its final citable form. Please note that during the production process errors may be discovered which could affect the content, and all legal disclaimers that apply to the journal pertain.

ATPase 2a (SERCA2a), is central to cardiac contraction and relaxation (10). This process is tightly regulated by reversible phosphorylation of a SR targeted protein phospholamban (PLN), a key negative regulator for SERCA2a activity(11). PLN phosphorylation by PKA at the Ser-16 site and by CaMKII at the Thr-17 site releases its inhibition to SERCA2a activity, resulting in elevated SR Ca<sup>2+</sup> uptake and accelerated intracellular Ca<sup>2+</sup> decline during relaxation. This is a major mechanism contributing to the enhanced contractility in response to adrenergic and other stimulation (12). In addition to its fundamental role in mediating myocyte contraction, PLN mediated Ca<sup>2+</sup> regulation also plays a crucial role in cardiomyocyte cell death regulation, especially following myocardial infarction (MI) (13). Depressed SR Ca<sup>2+</sup> cycling in the post-MI heart contributes to intracellular Ca<sup>2+</sup> overload which in turn leads to myocyte necrosis and apoptosis (14,15). Comparing to our extensive studies of the protein kinases involved in PLN regulation, our insights to PLN specific phosphatases responsible for its dephosphorylation are relatively limited. Previous studies have revealed that PP1, a relatively non-selective ser/thr protein phosphatase, contributes to a significant level of PLN phosphorylation regulation at both Ser-16 and Thr-17 sites (11,16-18). In addition, PP2A subunit B56 also mediates targeted dephosphorylation of PLN Ser-16 in addition to other cardiac proteins. PLN hypo-phosphorylation is a common molecular feature in the failing hearts and mutations of PLN that affect its phosphorylation and interaction with SERCA2a lead to cardiomyopathy in human (16,17,19- 25). Therefore, there is a need to better understand the underlying mechanism for PLN desphosphorylation and the relevant proteins.

In this report, we characterized an ER targeted member of the protein phosphatase 2C family, PP2Ce, in heart. PP2Ce mRNA was detected in heart. In cardiomyocytes and cell-free system, PP2Ce showed high specificity towards the Thr-17 site of PLN, and its expression significantly suppressed  $\beta$ -adrenergic stimulation induced calcium transients and exacerbated cell death upon oxidative stress. Expression of PP2Ce mRNA was found to be elevated in human cardiomyopathy hearts, and its protein was shown to be acutely induced in myocytes by pathological stressors via modulation of protein homeostasis. Cardiac specific expression of PP2Ce in a transgenic mouse model led to hypo-phosphorylation of PLN associated with exacerbated cardiac dysfunction and injury following ischemia/reperfusion. Therefore, PP2Ce is a novel SR membrane targeted and specific phosphatase for PLN in cardiomyocytes and its induction under pathological conditions may have a significant contribution to PLN hypophosphorylation, cardiomyocyte dysfunction and death.

## METHODS AND MATERIAL

### Generation of cardiac specific and inducible PP2Ce mice (PP2Ce TG)

Double transgenic PP2Ce mice were generated by crossing PP2Ce single transgenic line to strain carrying the tetracycline-controlled transactivator gene (tTA), which is under the regulation of alpha-myosin heavy chain promoter. Enhanced PP2Ce expression was achieved upon withdrawal of Doxycycline. Control animals used in this study were littermate mice carrying single transgenic tTA. Age between 10-15 weeks old male mice were used in the present study. All experiments were conducted in accordance with University of California, Los Angeles animal welfare guidelines.

### **Echocardiography**

Mice were anesthetized with 1% isoflurane. Echocardiography was taken and quantified on two dimension M-mode along short-axis of left ventricle using the Vevo 770 system and analyzed using the software suite provided by the Vendor (VisualSonics, Canada).

### **Isolation of Adult Cardiomyocytes and Measurement of Ca<sup>2+</sup> Transients**

Rat adult ventricular cardiomyocytes were enzymatically isolated in the following procedure. Hearts were quickly removed and retrogradely perfused with Ca<sup>2+</sup> free Tyrode's buffer containing collagenase II until hearts became softer (~10min). Calcium transients recording and measurement were performed as previously described (26).

### **Ischemia/Reperfusion (I/R) in Isolated Heart**

Ex vivo I/R model was performed as previously described (27). Briefly, heart was perfused in Langendorff system at a constant pressure of 80 mmHg by gravity. A fluid-filled balloon was inserted into the left ventricle and connected to a pressure transducer for continuous recording of left ventricular pressure and heart rate. After 30 min of stabilization, hearts were subjected to 30 min of global normothermic (37 °C) ischemia followed by up to 120 min of reperfusion. Heart tissues were collected for further studies. Infarct size measurement was performed by TTC staining and apoptosis positive cell were characterized by TUNEL staining.

### **cDNA Synthesis and Quantitative Real-Time PCR Analysis**

Total RNA was extracted from left ventricle with TRIzol reagent (Invitrogen) according to manufacturer's instruction. Five micrograms of total RNA was used to reverse-transcribe the first-strand cDNA with a Superscript first-strand synthesis kit (Invitrogen). cDNA transcripts were quantified by the iCycler iQ real-time PCR detection system using iQ SYBR Green Supermix (Bio-Rad, Hercules). GAPDH mRNA was used for normalization. Each reaction was performed in duplicate.

### **Western blot and Immunoprecipitation assay**

Western blots were performed as described previously (26). A total of 10 to 50 µg of total protein from ventricles and myocytes was loaded on 4% to 12% Bis-Tris gel, followed by electric transfer to nitrocellulose membranes. All protein signals were digitally recorded and quantified based on intensities, presented as average ± standard deviations.

### **In vitro dephosphorylation assay**

Left ventricle tissue extract was prepared in lysis buffer (50mM Tris-HCl (pH7.4), 150mM NaCl, 1% Nonidet P-40, and 1mM PMSF) with complete protein inhibitors (Roche Diagnostics) and incubated with 1µg of monoclonal anti-phospholamban antibody (Thermo Scientific) for 2h at 4 °C. The tissue lysate then was incubated with 60µg of protein A/G-agarose for 2h at 4 °C. After washing four times with washing buffer (20mM Tris-HCl(pH7.4), 150mM NaCl, and 1% Nonidet P-40), the beads were incubated with 2µg of GST or GST fusion protein in 20µl of reaction buffer containing 20mM HEPES(pH7.4), 20mM MgCl<sub>2</sub>, 2mM dithiothreitol, and 200µM ATP at 37 °C for 1h. The reaction was

terminated by adding NuPAGE LDS sample buffer (Invitrogen) containing 10%  $\beta$ -mercaptoethanol and boiling for 10min. Samples were subjected to SDS-PAGE.

### Assessment of Infarct Area

After 120 min of reperfusion, hearts were perfused with a triphenyltetrazolium chloride (TTC, 1%) solution for 5 min and frozen at  $-20^{\circ}\text{C}$ . The hearts were sliced into 6 (1mm of thickness/slice) cross sections. Viable myocardium showed red, and the infarct area showed pale white. Each slice image was recorded digitally using a camera mounted on a dissecting scope. The total and infarct area of ventricle of each slice were visually demarcated and measured using SPOT image analysis software. The relative infarction was calculated as a percentage infarcted area over the total ventricular area.

### TUNEL Staining

To detect apoptotic cells, a TUNEL assay was performed using the Apoptag kit (Invitrogen). Cross sections (5  $\mu\text{m}$ ) from frozen hearts (6 sections /heart) were prepared. Nuclei were counterstained with 4,6-diamidino-2-phenylindole (DAPI) and cardiomyocytes were labeled with  $\alpha$ -actin and the percentage of TUNEL-positive cardiomyocytes cells was calculated from total TUNEL positive myocyte nuclei vs. total DAPI labeled myocyte nuclei .

### MTT assay

NRVM were plated out in 100ul of medium at a concentration of  $5 \times 10^4$  cells in 96-well culture plates and cultured in an incubator at 37 degree in an atmosphere of 5%  $\text{CO}_2$  in air. After 36 hours of adenovirus infection, NRVM were treatment with hydrogen peroxide ( $\text{H}_2\text{O}_2$ : 20, 50,100  $\mu\text{Mol/L}$  for 16 hours; or 100  $\mu\text{Mol/L}$  of  $\text{H}_2\text{O}_2$  for 2, 8 and 16 hours. 10ul of 3-(4, 5-dimethylthiazol-2-yl)-2, 5-diphenyltetrazolium bromide (MTT,5mg/ml, dissolved in PBS) was added to each well. After 3 hours incubation in the dark, NRVM were washed and lysed to release formazan, which were subsequently dissolved in 100ul of DMSO. The absorbance was recorded in a microplate reader (Synergy<sup>TM</sup> H1, BioTek Instrument, Inc., Vermont, USA) at a wavelength of 570nm. Results were normalized for the control group.

### Statistical Analysis

Data were presented as mean  $\pm$  SD. Means between two experimental groups were compared with an unpaired Student *t* test or Mann-Whitney's U test. Multigroup comparisons were performed by Kruskal-Wallis test, two-way ANOVA, and repeated measure ANOVA. Multiple comparisons were performed by Stell method and Bonferroni correction.  $p < 0.05$  was considered statistically significant.

## RESULTS

### Identification of PP2Ce as an ER/SR membrane targeted protein phosphatase in cardiomyocytes

In previous studies, we reported a member of the Protein Phosphatase 2C family, PP2Ce, with targeted localization on the endoplasmic reticulum (ER) membrane (28,29) (Figure 1A). In fat cells and mammary gland, PP2Ce possesses highly specific activity towards

IRE1, a key signal molecule for ER stress response and serves as a negative feedback modulator to ER stress signaling with significant role in adiposity and lactating activity (28,29). By Northern blot analysis from tissues of adult mice, PP2Ce mRNA was also detected at substantial levels in brain, heart and diaphragm (Figure 1B). Using immunofluorescent microscopy, we confirmed that the full-length PP2Ce protein was specifically targeted on the SR membrane in adult rat cardiomyocytes, co-localizing with the Sarcoplasmic Reticulum Calcium ATPase 2a (SERCA2a) (Figure 1C). Furthermore, PP2Ce mRNA level was elevated in human ischemia cardiomyopathy or dilated cardiomyopathy hearts comparing to the non-failing controls (Figure 1D). However, over-expressing PP2Ce in cultured neonatal rat ventricular myocytes (NRVM) did not significantly affect ER stress response pathway including phosphor-PERK and phosphor-eIF2 $\alpha$ , as well as BiP and Xbp1 expression under basal or oxidative stress (Figure 2B), while exhibited modest reduction in CHOP and activated Caspase 3.

### Function of PP2Ce in cardiomyocytes as a PLN specific phosphatase

Considering the fact that PP2Ce is an SR targeted protein phosphatase with substantial cardiac expression, we investigated the impact of PP2Ce expression on the phosphorylation of several SR membrane proteins in cardiomyocytes under basal or post-isoproterenol (ISO) treatment. As shown in Figure 3A and B, PP2Ce expression did not markedly affect ryanodine receptor 2 (RyR2) phosphorylation at either PKA (Ser-2808) or CaMKII (Ser-2814) targeted sites or the phosphorylation levels of other cytosolic proteins such as troponin I. In contrast, PP2Ce expression potentially blocked ISO-induced PLN phosphorylation at the Thr-17 residue, and with relatively more modest effect on its Ser-16 phosphorylation under the same condition. To evaluate if PP2Ce induced PLN Thr-17 dephosphorylation was achieved by inhibiting CaMK activity or by directly targeting PLN, we tested the impact of PP2Ce expression on CaMK activity. As shown in Figure 3A,B, PP2Ce expression did not markedly affect the basal or the ISO induced auto-phosphorylation levels of CaMKII. Furthermore, when we co-expressed PP2Ce and a constitutively active form of CaMKII (CA) in NRVM, the PLN Thr-17 phosphorylation induced by the CaMKII-CA expression was markedly abolished (Figure 3C), further supporting PLN as a molecular target of PP2Ce. To demonstrate the direct phosphatase activity of PP2Ce towards PLN, we expressed a phosphatase dead mutant (D302A) (Figure 4A) and deletion mutant PP2Ce without ER targeting ability (1-57) in NRVM (Figure 4B) and these PP2Ce mutants showed no marked effect on PLN phosphorylation under ISO stimulation. These data suggest PP2Ce mediated PLN dephosphorylation requires both phosphatase activity and ER membrane localization. To further support its direct function and specificity, we generated recombinant GST-fusion proteins for the wild-type and a phosphatase dead mutant of PP2Ce, and incubated the recombinant PP2Ce or PP2Ce-mutant proteins with PLN proteins prepared by immunoprecipitation from ISO treated mouse left ventricle tissues where both Ser-16 and Thr-17 sites were highly phosphorylated. In this cell-free system, PP2Ce did not affect PLN phospho-Ser-16 level but effectively diminished the phospho-Thr-17 level (Figure 4C), supporting that dephosphorylating the PLN-Thr-17 is a direct and specific intrinsic activity of PP2Ce. Finally, by co-immunoprecipitation assay, we demonstrated protein-protein interaction between PLN and PP2Ce in intact mouse hearts (Figure 4D). All

these data suggest that PP2Ce is a novel PLN phosphatase with a highly specific intrinsic phosphatase activity towards phosphor-Thr-17.

### Post-transcriptional Regulation of PP2Ce Expression in Cardiomyocytes

Since there is no commercial antibody sufficiently sensitive to detect the endogenous PP2Ce protein in cardiomyocytes, we followed the expression of PP2Ce-Flag fusion protein introduced into NRVM (Figures 3-5). Stimulation of NRVM with ISO significantly and consistently induced PP2Ce protein level as early as 2 hours after treatment (Figures 3B). This induction is specific to PP2Ce as ectopic expression of GFP or another PP2C family member, PP2Ca using the same expression vectors were not affected by ISO treatment within the same time period (Figure 3B and 5A). The ISO mediated induced of PP2Ce protein was significantly blunted by protein synthesis inhibition (Figure 5B, C) but further increased by short-term proteasome inhibition (Figure 5B, C). Therefore, ISO mediated PP2Ce induction involved protein synthesis and degradation. Direct induction of cAMP by forskolin treatment was sufficient to induce the same pattern of PP2Ce protein increase (Figure 5D). However, PKA inhibition by treating cells with H89 markedly blocked ISO mediated PP2Ce induction (Figure 5E). In addition to  $\beta$ -adrenergic-stimulation, oxidative stress induced by superoxide treatment also increased PP2Ce protein level in cardiomyocytes as early as 8 hours (Figure 2A, B). All these evidences suggest that PP2Ce protein is subject to dynamic regulation at protein in response to pathological stressors in cardiomyocytes. Such induction can serve as an intrinsic and local negative modulator for  $\beta$ -adrenergic signaling by specifically targeting to PLN Thr-17 phosphorylation.

### Functional Impact of PP2Ce in Cardiomyocytes

As we established PLN as a specific substrate of PP2Ce and a key modulator of SR calcium homeostasis, we investigated the physiological impact of PP2Ce on SR calcium cycling in cardiomyocyte. We measured the impact of PP2Ce expression on SR calcium cycling in isolated adult rat ventricular cardiomyocytes. As shown in Figure 6, expression of PP2Ce did not affect basal calcium transient but significantly reduced the intracellular peak calcium amplitude and slowed the calcium transient decline rate following ISO stimulation, supporting the functional impact of PP2Ce expression on SR calcium cycling consistent with its targeted dephosphorylation of PLN.

To further determine the functional role of PP2Ce in intact heart, we developed a transgenic mouse model with cardiac specific expression of PP2Ce (PP2Ce-TG) (Figure 7A). Western-Blots revealed that PP2Ce expression was induced in the transgenic heart specifically in double transgenic animals (Figure 7B). Consistent with previous *in vitro* observations, at basal level, the PP2Ce-TG mice exhibited normal cardiac phenotype at morphological and functional levels (Table 1). Also consistent with the *in vitro* results, the basal PLN phosphorylation at Thr-17 was significantly inhibited, although in this case, Ser-16 phosphorylation was also reduced (Figure 7C, D). In contrast, the phosphorylation levels of RyR2 at both PKA and CaMKII dependent sites, and the phosphorylation levels of troponin I were not changed, nor were the total protein levels for RyR2, troponin I, SERCA-2a and sodium-calcium exchanger 1 (NCX1) (Figure 7C and D). Notably, PP1 expression was not affected by PP2Ce expression. In isolated intact left ventricular cardiomyocytes loaded with

Fluo-4 AM ( $\text{Ca}^{2+}$  fluorescent dye) and paced at 1 Hz by electric stimulator (Figure 7E), the 50% decay time of  $\text{Ca}^{2+}$  transients was significantly prolonged in the PP2Ce-TG myocytes (average at 159.4 milliseconds) relative to the non-TG controls (average at 135.9 milliseconds,  $p < 0.05$ ). However, there were no significant differences in the peak  $\text{Ca}^{2+}$  transient amplitude or the time to peak of  $\text{Ca}^{2+}$  transients between the PP2Ce-TG myocytes vs. controls (Figure 7E).

### PP2Ce Expression Impairs Inotropic Response to Isoproterenol

To directly examine the functional impact of PP2Ce expression on cardiac contractile function and isoproterenol response, we measured left ventricular pressure in isolated perfused hearts from non-transgenic and PP2Ce transgenic mice. As shown in Figure 8, the PP2Ce transgenic hearts had similar contractile function at basal condition (Figure 8 and Table 2), but showed blunted response to isoproterenol stimulation comparing to wildtype control hearts based on systolic pressure,  $\text{dP/dT}_{\text{max}}$  and  $\text{dP/dT}_{\text{min}}$ , as well as developed pressure (LVDP) (Figure 8B). This is consistent with *in vitro* calcium measurement observed in isolated myocytes (Figure 7).

### PP2Ce Expression Reduced Function Recovery Post Ischemia/Reperfusion Injury

CaMKII mediated Thr-17 phosphorylation of PLN has been implicated in ischemia/reperfusion (I/R) injury and cardiomyocyte death regulation (13-15). Therefore, we investigated the effect of PP2Ce expression in the intact PP2Ce-TG hearts during I/R injury. Using *Langendorff* preparation, the isolated mouse hearts from the PP2Ce-TG and the Control mice were subjected to 30 minutes of global no-flow ischemia followed by 60 to 120 min of reperfusion (I/R) while contractility was continuously monitored via a conductance catheter for left ventricle pressure (Figure 9A). As shown in Figure 9B, the functional recovery following reperfusion was significantly impaired in the PP2Ce-TG transgenic hearts compared with the Controls. Particularly, after 45 minutes of reperfusion, systolic function as measured from left ventricle developed pressure (LVDP) (PP2Ce-TG vs. control:  $39.33 \pm 11.64$  mmHg vs.  $55.79 \pm 8.3$  mmHg,  $p < 0.01$ ) (Figure 9B) and  $\text{dP/dT}_{\text{max}}$  (PP2Ce-TG vs. control:  $1839.78 \pm 410.98$  mmHg/s vs.  $2905.99 \pm 490.76$  mmHg/s,  $p < 0.01$ ) was significantly reduced in the PP2Ce-TG hearts compared to the Controls (Figure 9A-D, Table 2). In addition, cardiac relaxation as measured from  $\text{dP/dT}_{\text{min}}$  (PP2Ce-TG vs. control:  $1274.42 \pm 239.59$  mmHg/s vs.  $1707.4 \pm 190.53$  mmHg/s,  $p < 0.05$ ) (Figure 9D) and  $\tau$  (PP2Ce-TG vs. control:  $46.7 \pm 21.4$  ms vs.  $23.3 \pm 5.5$  ms,  $p < 0.05$ ) (Figure 9E) were also significantly impaired in the PP2Ce-TG hearts compared with the controls at 60 minutes post reperfusion. These data demonstrated exacerbated systolic and diastolic dysfunction following I/R injury upon PP2Ce expression in heart. Along with impaired functional recovery, myocardial infarct size as measured by TTC staining (infarct area vs. area at risk (AAR)) at 120 minutes post reperfusion was significantly larger in the PP2Ce-TG hearts compared with the Controls (IA/AAR:  $59.82 \pm 6.1$  vs  $40.06 \pm 6.71$ ,  $p < 0.01$ ) (Figure 10A,B). Additionally, using TUNEL staining, more apoptotic cells were detected in the PP2Ce-TG heart than the Control hearts (Figure 10C). To further support the status of impaired cardiac protection by PP2Ce expression, mitochondrial-mediated apoptotic cell death signaling as represented by cleaved caspase 9 was detected to be significantly induced in the PP2Ce-TG hearts compared to Controls following I/R (Figure 10D, E).

## PP2Ce Expression Promotes Oxidative Stress Induced Cell Death in Cardiomyocytes

We next investigated whether PP2Ce expression directly affects myocyte survival under oxidative stress *in vitro*. NRVMs showed dosage dependent cell death following H<sub>2</sub>O<sub>2</sub> treatment at 20, 50, 100 μM for upto 16 hours based on MTT assay. Following PP2Ce expression, the NRVM showed significantly reduced cell viability upon H<sub>2</sub>O<sub>2</sub> or ionomycin treatment compared with the GFP expressing cells (Figure 11A and B). To explore signaling mechanism involved in this process, we examined AKT and MAP kinase pathways. As shown in Figure 11C and D, PP2Ce expression significantly reduced pro-survival AKT and ERK activity following oxidative stress without significantly impacting on pro-death stress-MAPK activities, including p38 and JNK. In line with the role of PP2Ce in SR calcium regulation, calcium overload induced cell death triggered ionomycin treatment for 24 hours was also significantly enhanced by PP2Ce expression (Figure 11B). Taken together, PP2Ce expression promotes oxidative injury via enhanced myocyte death associated with disturbance in intracellular signaling.

## DISCUSSION

In this report, we characterized a newly identified protein phosphatase PP2Ce in cardiomyocytes in terms of its molecular target and cellular/physiological function in heart. Our findings establish that PP2Ce is localized on the sarcoplasmic reticulum (SR) membrane overlapping with SR calcium ATPase 2a. PP2Ce expression is significantly induced at mRNA level in human failing hearts while PP2Ce protein, when expressed in cardiomyocytes, is acutely induced by β-adrenergic stimulation and oxidative stress. From extensive molecular and cellular studies, we find PP2Ce is a highly specific PLN phosphatase with intrinsic activity towards PLN Thr-17. Expression of PP2Ce in cardiomyocytes showed a significant impact on SR calcium homeostasis, particular in calcium uptake, in line with its targeted dephosphorylation of PLN. In addition, PP2Ce expression both *in vitro* and *in vivo* promoted oxidative injury and myocyte death. Therefore, PP2Ce functions as an uncharacterized modulator for cardiac calcium cycling and has a potentially significant contribution to stress adaption in heart in response to β-adrenergic stimulation and oxidative injury.

PP2Ce protein is increased within 2 hours in response to acute β-adrenergic stimulation at protein level. PP2Ce protein is also affected by short-term proteasome inhibition alone, and ISO induced PP2Ce protein induction requires *de novo* protein synthesis. Therefore, PP2Ce protein homeostasis is modulated by both synthesis and proteasome dependent degradation at basal state. The underlying mechanism of its turn-over is unclear and the molecular signaling participated in ISO mediated PP2Ce protein induction remains to be established although our data suggest that it is a PKA dependent process. Interestingly, similar induction was observed in oxidative stressed myocytes, suggesting such induction can be triggered by different stressors through different pathways. Induction of a PLN specific phosphatase in cardiomyocytes following pathological stress offers an intriguing mechanism of negative feedback regulation in cardiomyocyte to maintain SR calcium homeostasis following stress stimulations (Figure 12). Significant induction of PP2Ce expression detected in human failing hearts may represent a chronic maladaptation similar to β-adrenergic desensitization.



We showed in cell-free system, PP2Ce specifically dephosphorylated the Thr-17 site of PLN but not the Ser-16 site and PP2Ce expression did not affect the phosphorylation status of other ER membrane targeted proteins, such as RyR. This implies that PP2Ce possesses a very high degree of intrinsic substrate specificity. This is in contrast to protein phosphatase 1 (PP1), a major PLN phosphatase with specificity towards both Ser-16 and Thr-17 sites, as well as other substrates. In addition, PLN dephosphorylation can also be carried out by PP2A with its regulatory subunit B56. However, the specificity of PP2A/B56 is also not limited to PLN. In intact heart, however, PP2Ce expression affected both Ser-16 and Thr-17 sites, suggesting either PP2Ce acquires new specificity in adult cardiomyocytes due to yet to be characterized complex interaction or indirectly regulates Ser-16 phosphorylation. Nevertheless, targeted PLN dephosphorylation *in vivo* is consistent with the phenotype observed in the PP2Ce-TG hearts which displayed relatively normal basal contractile function but showed blunted inotropic response to ISO stimulation and more susceptibility to ischemia/reperfusion induced injury. In fact, our observation is in good agreement with previous findings that CaM kinase mediated PLN regulation (through Thr-17 phosphorylation) affects cardiac injury following ischemia/reperfusion. PP2Ce is also reported to regulated IRE1 mediated unfold-protein response by specifically interact and dephosphorylate IRE1 without cross-reactivity towards PERK. In heart, basal IRE1 expression is low (undetectable with current antibodies, data not shown) while the PP2Ce expression is relatively abundant. Therefore, PP2Ce function in heart may involve both of these substrates or other yet to be characterized substrates. Further molecular studies will be needed to determine all possible downstream targets of PP2Ce in heart, and to uncover the underlying molecular basis for such a high substrate specificity. In summary, our extensive molecular, cellular and molecular analyses have revealed a previously uncharacterized signaling regulator in heart, an ER membrane targeted protein phosphatase with high specificity towards PLN Thr-17 phosphorylation. Its induction in human failing hearts and our *in vivo* evidence from intact mouse heart implicate its potential role in pathogenesis of cardiac injury through modulating SR calcium uptake and homeostasis.

## Perspectives

Cardiac dysfunction is significantly contributed by defects in cardiomyocyte calcium homeostasis and cycling. Phospholamban (PLN) is a key regulator of SR calcium ATPase (SERCA) and its function is modulated by PKA and CaMKII mediated protein phosphorylation, and loss of PLN phosphorylation is a molecular hallmark associated with heart failure. PP2Ce is a newly identified phosphatase with potent and specific activity to dephosphorylate PLN in cardiomyocytes. PP2Ce expression is induced rapidly following pathological stress and PP2Ce induction negative impacts on cardiac contractile function and cardiomyocyte viability. Therefore, PP2Ce induction may represent a novel mechanism for heart failure, and its inactivation can serve as a potential therapeutic strategy.

## Acknowledgments

This work is supported in part by grants from National Institutes of Health R01HL108186 (H.R., Y.W.) and R01 HL070079 (Y.W.), from the Ministry of Education, Culture, Sports, Science and Technology of Japan (S.M. and T.A.), the Vehicle Racing Commemorative Foundation (S.M.), The Jikei University Graduate Research Fund (SM), and the MEXT Supported Program for the Strategic Research Foundation at Private Universities (S.M. and T.A.). This no industry relationship associated with this study.

## References

1. Thomas NL, George CH, Lai FA. Role of ryanodine receptor mutations in cardiac pathology: more questions than answers? *Biochem Soc Trans.* 2006; 34:913–8. [PubMed: 17052226]
2. Jiang D, Xiao B, Yang D, et al. RyR2 mutations linked to ventricular tachycardia and sudden death reduce the threshold for store-overload-induced Ca<sup>2+</sup> release (SOICR). *Proc Natl Acad Sci U S A.* 2004; 101:13062–7. [PubMed: 15322274]
3. Periasamy M, Kalyanasundaram A. SERCA pump isoforms: their role in calcium transport and disease. *Muscle Nerve.* 2007; 35:430–42. [PubMed: 17286271]
4. Tiso N, Stephan DA, Nava A, et al. Identification of mutations in the cardiac ryanodine receptor gene in families affected with arrhythmogenic right ventricular cardiomyopathy type 2 (ARVD2). *Hum Mol Genet.* 2001; 10:189–94. [PubMed: 11159936]
5. Periasamy M, Reed TD, Liu LH, et al. Impaired cardiac performance in heterozygous mice with a null mutation in the sarco(endo)plasmic reticulum Ca<sup>2+</sup>-ATPase isoform 2 (SERCA2) gene. *J Biol Chem.* 1999; 274:2556–62. [PubMed: 9891028]
6. Hovnanian A. SERCA pumps and human diseases. *Subcell Biochem.* 2007; 45:337–63. [PubMed: 18193643]
7. MacLellan WR. Advances in the molecular mechanisms of heart failure. *Curr Opin Cardiol.* 2000; 15:128–35. [PubMed: 10952417]
8. Elliott P, McKenna WJ. Hypertrophic cardiomyopathy. *Lancet.* 2004; 363:1881–91. [PubMed: 15183628]
9. Bers DM, Despa S, Bossuyt J. Regulation of Ca<sup>2+</sup> and Na<sup>+</sup> in normal and failing cardiac myocytes. *Ann N Y Acad Sci.* 2006; 1080:165–77. [PubMed: 17132783]
10. Eisner D. Calcium in the heart: from physiology to disease. *Exp Physiol.* 2014; 99:1273–82. [PubMed: 25128325]
11. MacLennan DH, Kranias EG. Phospholamban: a crucial regulator of cardiac contractility. *Nat Rev Mol Cell Biol.* 2003; 4:566–77. [PubMed: 12838339]
12. Haghghi K, Bidwell P, Kranias EG. Phospholamban interactome in cardiac contractility and survival: A new vision of an old friend. *J Mol Cell Cardiol.* 2014; 77:160–7. [PubMed: 25451386]
13. Iwanaga Y, Hoshijima M, Gu Y, et al. Chronic phospholamban inhibition prevents progressive cardiac dysfunction and pathological remodeling after infarction in rats. *J Clin Invest.* 2004; 113:727–36. [PubMed: 14991071]
14. Nakayama H, Chen X, Baines CP, et al. Ca<sup>2+</sup>- and mitochondrial-dependent cardiomyocyte necrosis as a primary mediator of heart failure. *J Clin Invest.* 2007; 117:2431–44. [PubMed: 17694179]
15. Vittone L, Mundina-Weilenmann C, Mattiazzi A. Phospholamban phosphorylation by CaMKII under pathophysiological conditions. *Front Biosci.* 2008; 13:5988–6005. [PubMed: 18508637]
16. Rodriguez P, Kranias EG. Phospholamban: a key determinant of cardiac function and dysfunction. *Arch Mal Coeur Vaiss.* 2005; 98:1239–43. [PubMed: 16435604]
17. Chu G, Kranias EG. Phospholamban as a therapeutic modality in heart failure. *Novartis Found Symp.* 2006; 274:156–71. discussion 172-5, 272-6. [PubMed: 17019811]
18. Waggoner JR, Kranias EG. Role of phospholamban in the pathogenesis of heart failure. *Heart Fail Clin.* 2005; 1:207–18. [PubMed: 17386847]
19. Minamisawa S, Sato Y, Tatsuguchi Y, et al. Mutation of the phospholamban promoter associated with hypertrophic cardiomyopathy. *Biochem Biophys Res Commun.* 2003; 304:1–4. [PubMed: 12705874]
20. Schmitt JP, Kamisago M, Asahi M, et al. Dilated cardiomyopathy and heart failure caused by a mutation in phospholamban. *Science.* 2003; 299:1410–3. [PubMed: 12610310]
21. Haghghi K, Kolokathis F, Pater L, et al. Human phospholamban null results in lethal dilated cardiomyopathy revealing a critical difference between mouse and human. *J Clin Invest.* 2003; 111:869–76. [PubMed: 12639993]

22. Haghghi K, Kolokathis F, Gramolini AO, et al. A mutation in the human phospholamban gene, deleting arginine 14, results in lethal, hereditary cardiomyopathy. *Proc Natl Acad Sci U S A*. 2006; 103:1388–93. [PubMed: 16432188]
23. DeWitt MM, MacLeod HM, Soliven B, McNally EM. Phospholamban R14 deletion results in late-onset, mild, hereditary dilated cardiomyopathy. *J Am Coll Cardiol*. 2006; 48:1396–8. [PubMed: 17010801]
24. Haghghi K, Chen G, Sato Y, et al. A human phospholamban promoter polymorphism in dilated cardiomyopathy alters transcriptional regulation by glucocorticoids. *Hum Mutat*. 2008; 29:640–7. [PubMed: 18241046]
25. Medin M, Hermida-Prieto M, Monserrat L, et al. Mutational screening of phospholamban gene in hypertrophic and idiopathic dilated cardiomyopathy and functional study of the PLN -42 C>G mutation. *Eur J Heart Fail*. 2007; 9:37–43. [PubMed: 16829191]
26. Ruan H, Mitchell S, Vainoriene M, et al. Gi alpha 1-mediated cardiac electrophysiological remodeling and arrhythmia in hypertrophic cardiomyopathy. *Circulation*. 2007; 116:596–605. [PubMed: 17646583]
27. Ruan H, Li J, Ren S, et al. Inducible and cardiac specific PTEN inactivation protects ischemia/reperfusion injury. *J Mol Cell Cardiol*. 2009; 46:193–200. [PubMed: 19038262]
28. Ren S, Lu G, Ota A, et al. IRE1 phosphatase PP2Ce regulates adaptive ER stress response in the postpartum mammary gland. *PLoS One*. 2014; 9:e111606. [PubMed: 25369058]
29. Lu G, Ota A, Ren S, et al. PPM1l encodes an inositol requiring-protein 1 (IRE1) specific phosphatase that regulates the functional outcome of the ER stress response. *Molecular metabolism*. 2013; 2:405–16. [PubMed: 24327956]

## ABBREVIATIONS

<b>PLN</b>	phospholamban
<b>SERCA2a</b>	sarcolemma-endoplasmic reticulum calcium ATPase 2a
<b>PP2Ce</b>	protein phosphatase 2C on ER membrane
<b>CaMKII</b>	calmodulin kinase II
<b>RyR2</b>	ryanodine receptor
<b>PP2A</b>	Protein Phosphatase 2A
<b>NRVM</b>	Neonatal rat ventricular myocyte
<b>GFP</b>	Green Fluorescent Protein

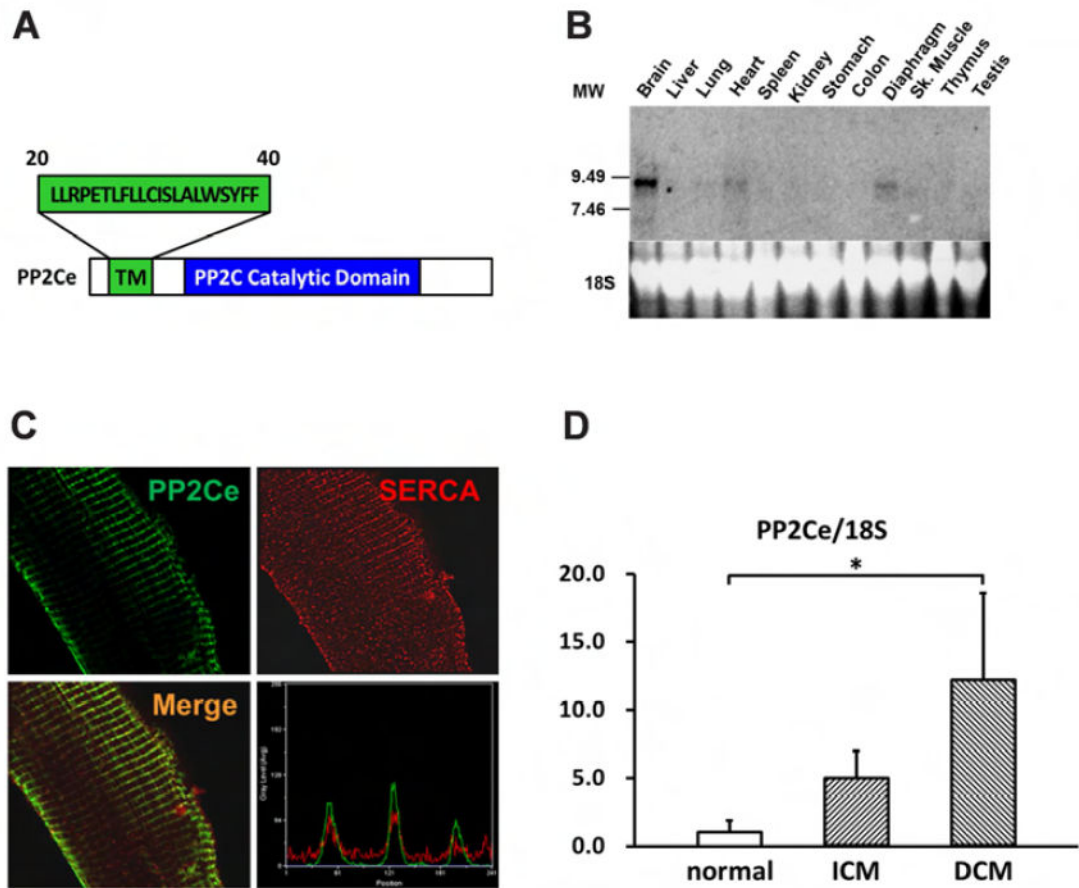
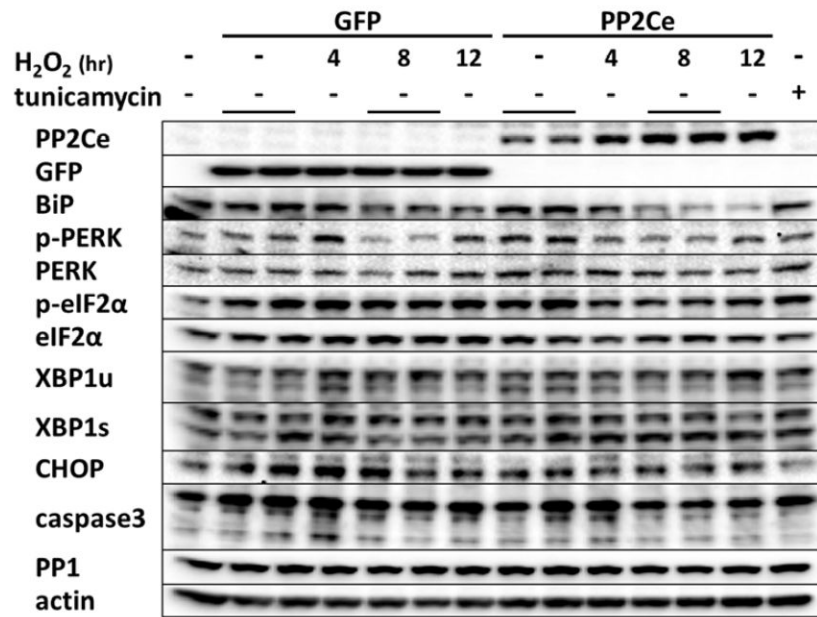


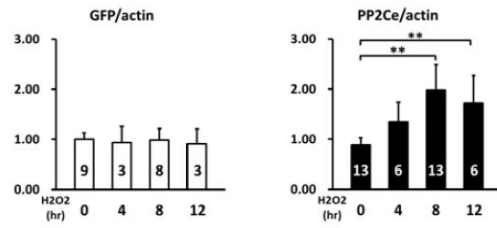
**Figure 1. PP2Ce is an ER membrane targeted protein phosphatase and detected in adult mouse hearts**

**A.** Schematic description of PP2Ce protein with signal peptide sequence (aa20-40), transmembrane domain, and conserved PP2C phosphatase activity domain highlighted. **B.** Northern-blot analysis of PP2Ce mRNA expression in different tissues from adult mice with significant expression detected in brain, heart and diaphragm. **C.** Immunohistochemistry results displayed PP2Ce (green) was co-localized with SERCA2a (red) in adult rabbit ventricular cardiomyocytes as supported in merged image and line-scanning intensity analysis. **D.** Relative expression of PP2Ce mRNA detected by qRT-PCR in heart samples from ischemic cardiomyopathy (ICM, n=3) and dilated cardiomyopathy (DCM, n=3) comparing with non-heart failure (normal, n=3). \*:  $p < 0.05$  vs. normal.

**A**



**B**



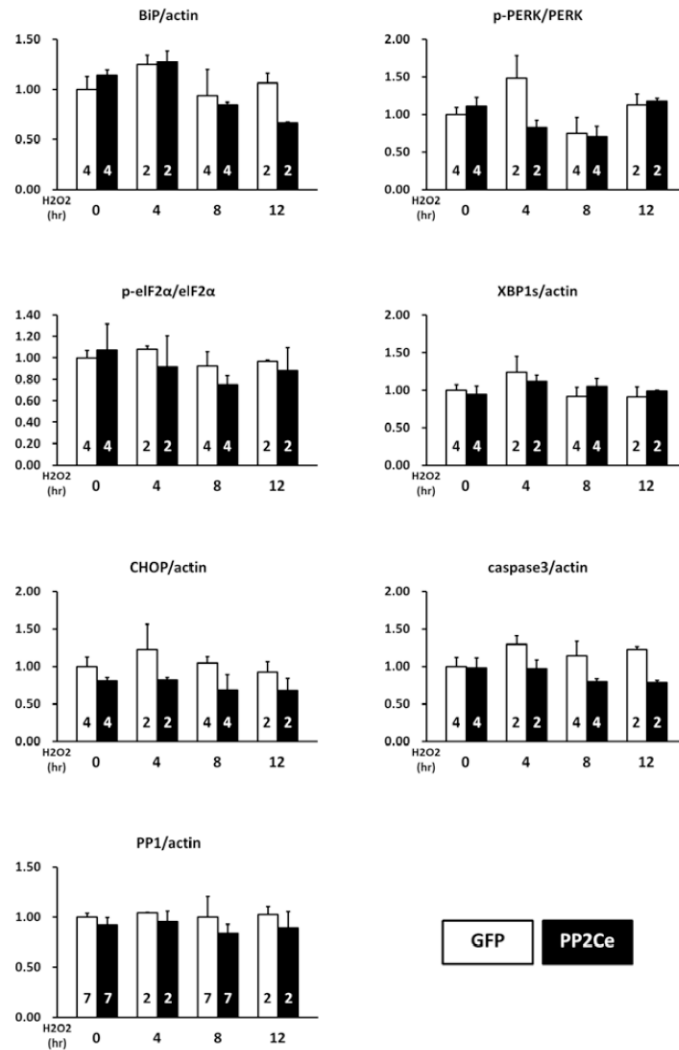
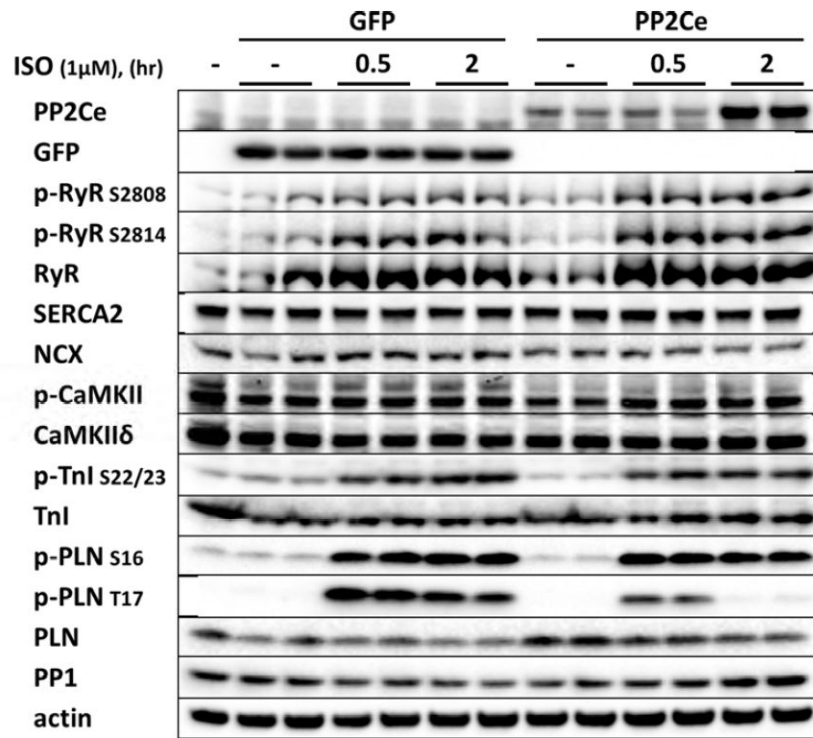


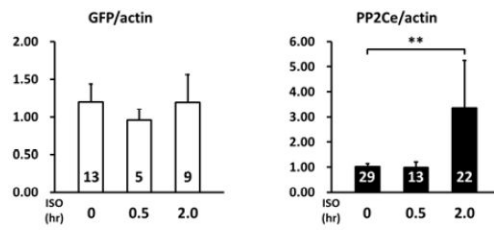
**Figure 2. PP2Ce expression on ER stress signaling pathway in NRVM**

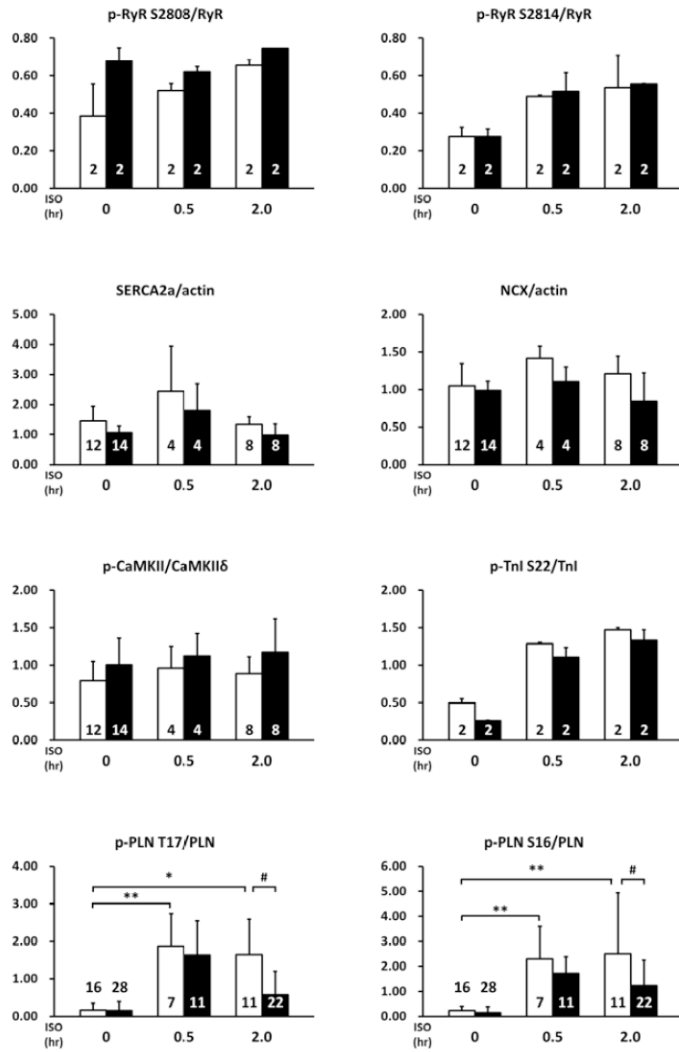
**A.** Representative immunoblot of ER stress regulators as indicated in NRVM expressing GFP and PP2Ce in response to 50μM H<sub>2</sub>O<sub>2</sub> treatment at specific time points as indicated. 5μg/ml tunicamycin treated NRVM was used as a positive control. **B.** Quantification of immunoblot signals with independent experimental replicate number labeled in each column. \*\*:  $p < 0.01$ .

**A**

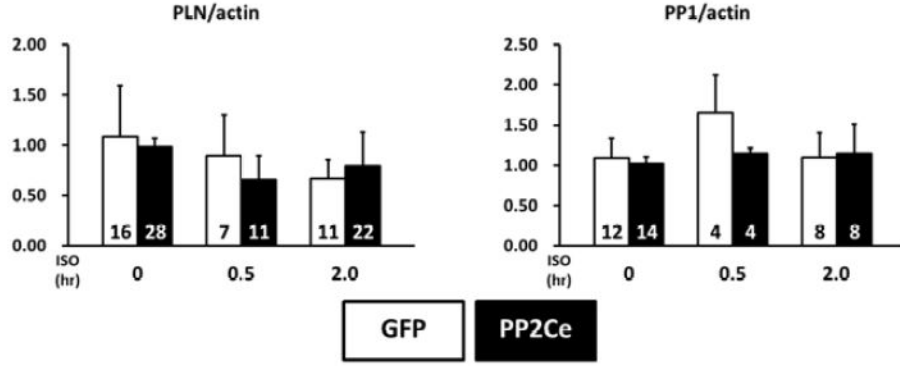


**B**









**C**

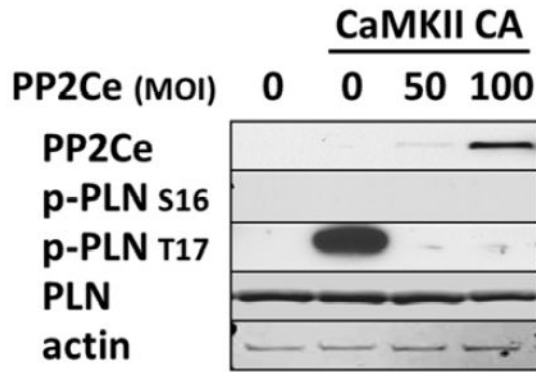


**Figure 3. PP2Ce is a specific phosphatase for PLN Thr-17 phosphorylation site**

**A.** Representative immunoblot from NRVM expressing GFP or PP2Ce were treated with 1 $\mu$ M isoproterenol for 0.5 and 2 hours as indicated. **B.** Quantification of immunoblot signals with independent experimental replicate number labeled in each corresponding columns. \*:  $p < 0.05$ , \*\*:  $p < 0.01$  vs. untreated. #:  $p < 0.05$  between PP2Ce and GFP at each time points. **C.** Western blot for NRVM co-expressing active CaMKII (CaMKII-CA) and increasing amount of PP2Ce as indicated.

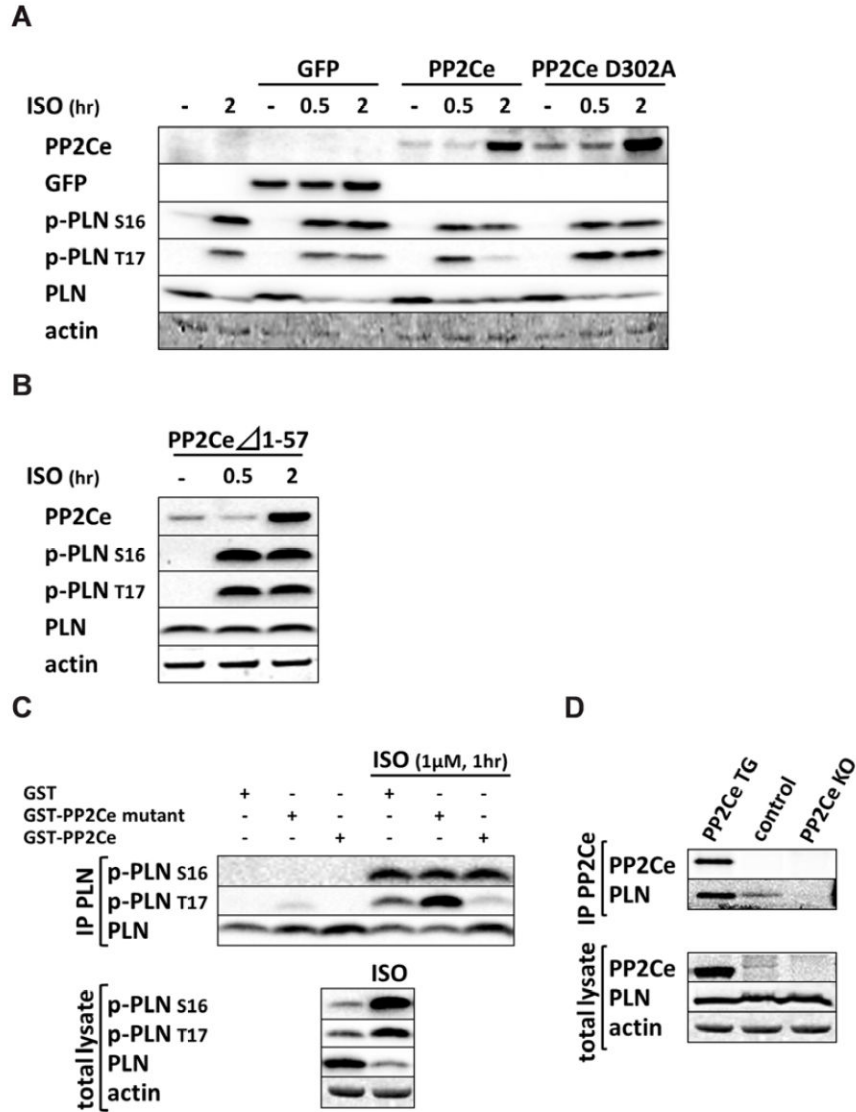


**Figure 4. Specificity of PP2Ce activity to PLN Thr-17 phosphorylation**

**A.** Immunoblot of PP2Ce, GFP, and PLN phosphorylation (Ser-16 and Thr-17) in NRVM expressing GFP or PP2Ce wildtype or PP2Ce phosphatase dead mutant (D320A) following 1 $\mu$ M isoproterenol treatment at different time points as indicated. **B.** ISO induced PP2Ce expression and PLN phosphorylation in NRVM expressing PP2Ce truncation mutant (1-57) which has lost ER targeting capacity ((28, 29)). **C.** PP2Ce–GST fusion protein was incubated with PLN isolated from NRVM with or without ISO treatment, followed by immunoblot for total and phosphorylation levels of PLN at Ser-16 and Thr-17. **D.** Co-immunoprecipitation of PP2Ce and PLN in mouse heart using PP2Ce TG and PP2Ce KO as positive and negative control, respectively.

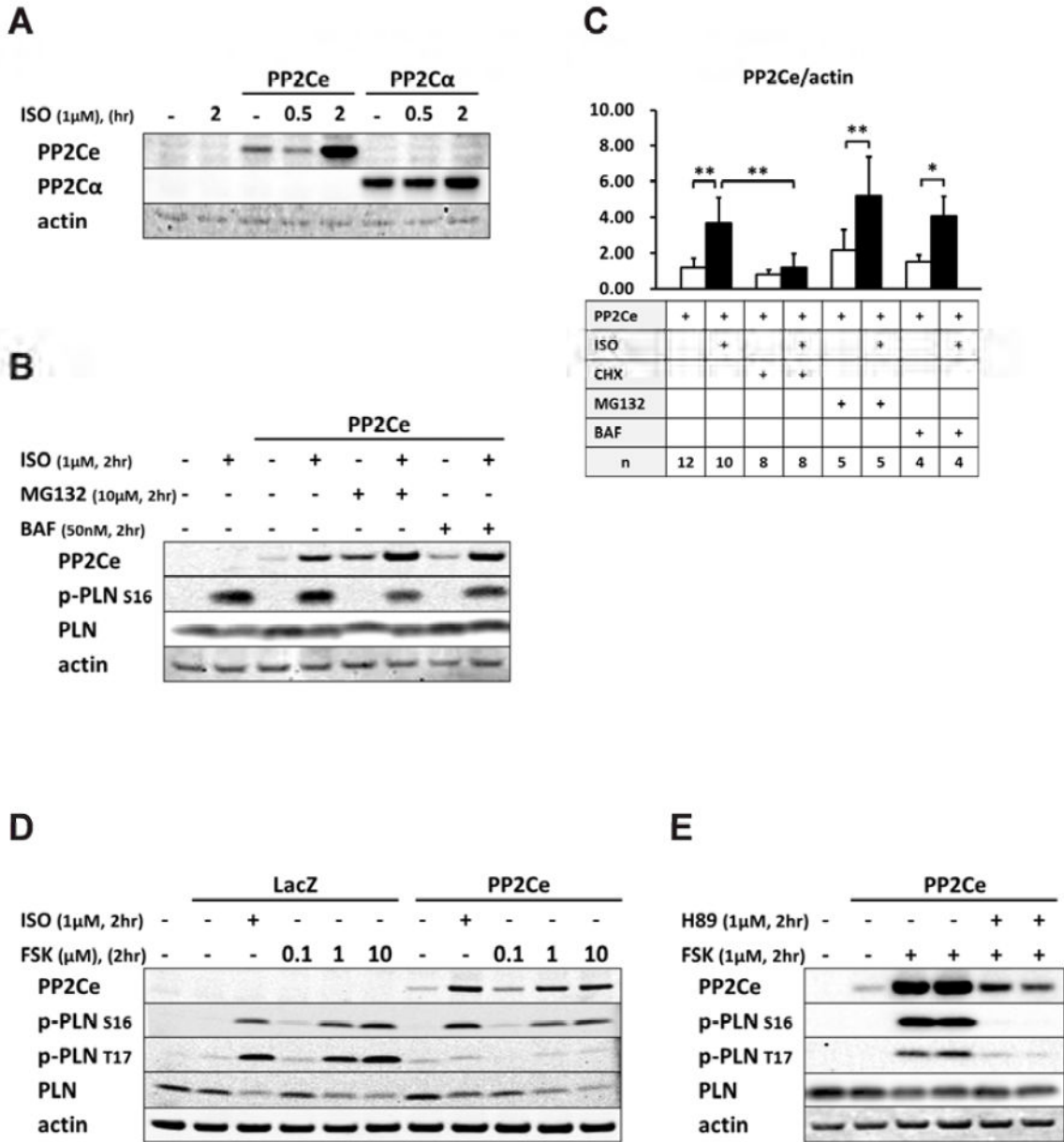


**Figure 5. ISO mediated regulation of PP2Ce protein in cardiomyocytes**

**A.** PP2Ce and PP2Cα expression in NRVM following ISO treatment. **B.** PP2Ce expression in NRVM treated with ISO (1μM) with or without co-treatment of proteasome inhibitor MG132 (10μM) or lysosomal inhibitor BAF (50nM) as indicated. **C.** Quantification of PP2Ce expression in NRVM treated with ISO with or without additional treatment of cycloheximide (CHX), MG132 or BAF as indicated. n: number of total experimental replicates, \*:  $p < 0.05$ , \*\*:  $p < 0.01$ . **D.** PP2Ce expression in NRVM treated ISO or forskolin (FSK) at 0.1, 1, and 10μM concentrations as indicated. **E.** PP2Ce expression in NRVM treated with FSK (1μM) with or without PKA inhibitor H89 (1μM) as indicated.

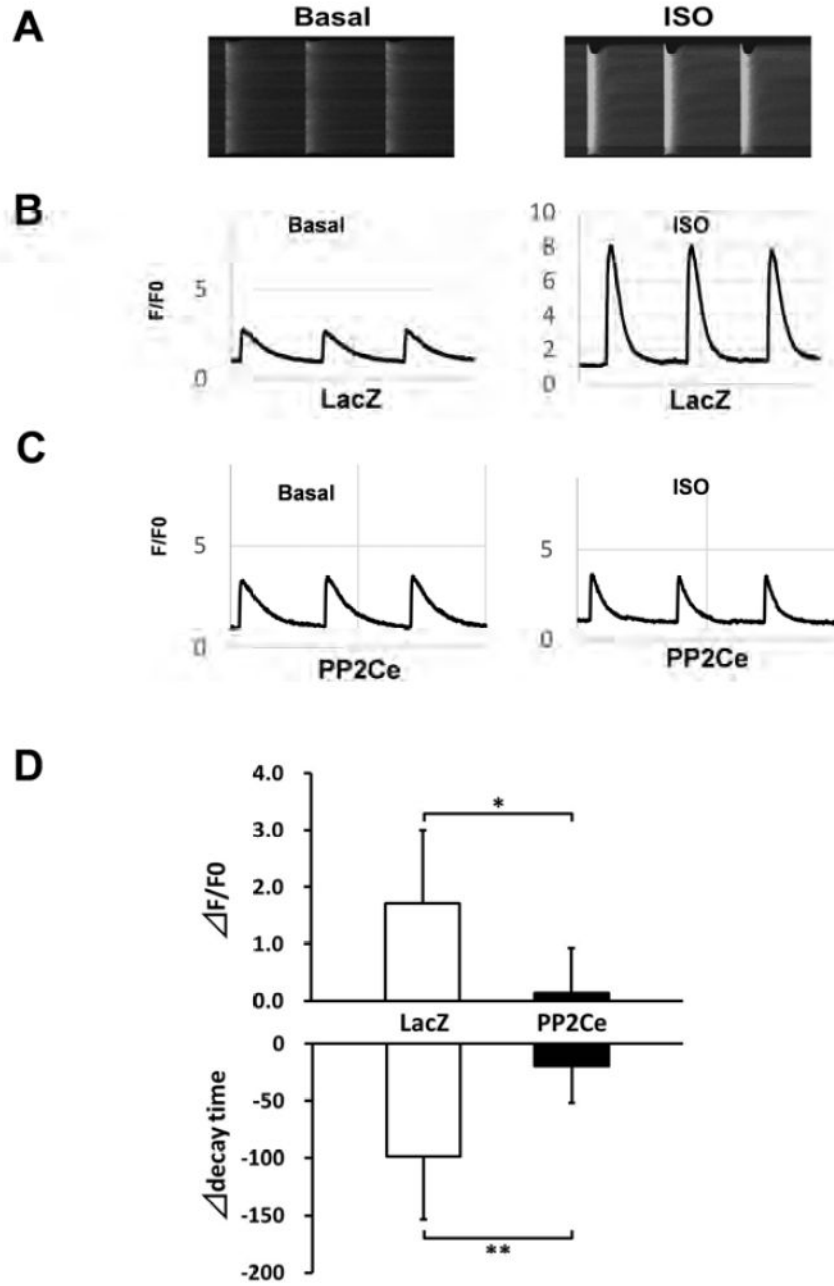


**Figure 6. Functional impact of PP2Ce expression on SR calcium homeostasis in adult rat cardiomyocytes**

**A.** Representative images of calcium transients from control rat myocytes at basal and following ISO (0.1 $\mu$ M) treatment; **B.** Representative recording of calcium signal (F/F<sub>0</sub>) at basal and post-ISO treatment in LacZ expressing rat adult cardiomyocytes. **C.** Representative recording of calcium signal at basal and post-ISO treatment in PP2Ce expressing rat adult cardiomyocytes. **D.** Summary data of changes in calcium amplitude and decay time in adult cardiomyocytes expressing LacZ (n=5) vs. PP2Ce (n=3) between basal

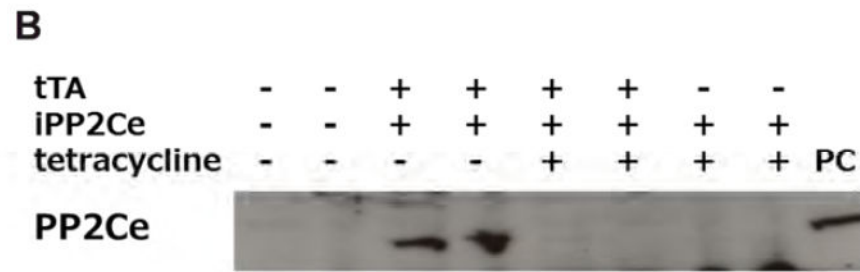
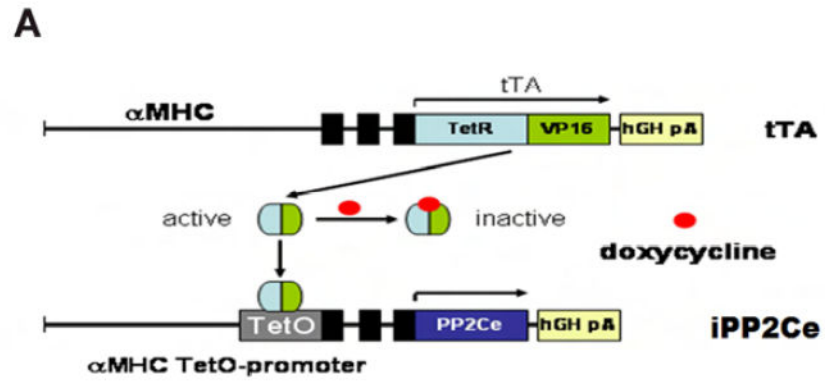
and post-ISO treatment. : the difference between post and pre ISO treatment. \*:  $p < 0.05$ , \*\*:  $p < 0.01$  LacZ vs. PP2Ce respectively.

Author Manuscript

Author Manuscript

Author Manuscript

Author Manuscript



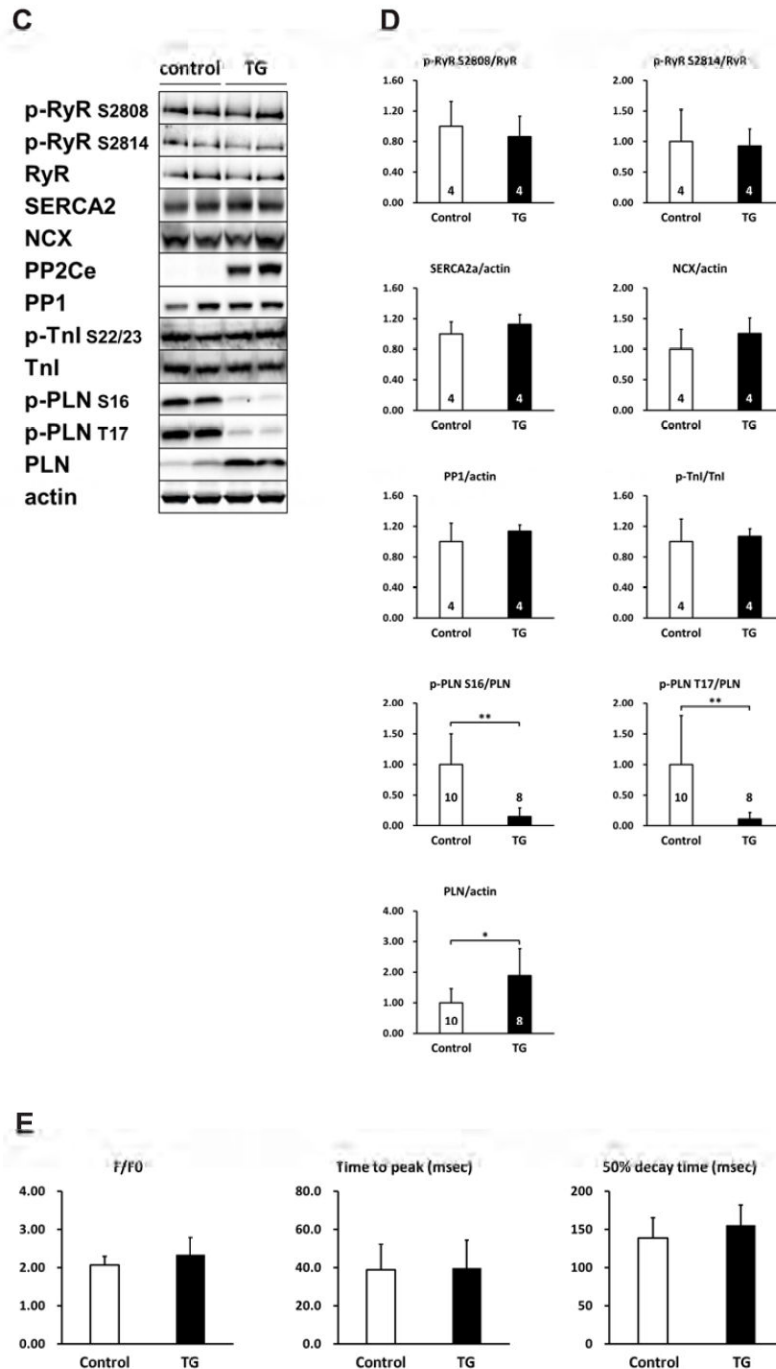


**Figure 7. Impact of PP2Ce on calcium homeostasis in intact mouse heart**

**A.** Schematic drawing of PP2Ce-transgenic mouse with tissue specific expression of PP2Ce in heart. **B.** PP2Ce protein expression in mouse hearts from four genotypes carrying either none, single or double transgenes of  $\alpha$ MHC-tTA expressing tet-off suppressor (tTA) and  $\alpha$ MHC-TetO-PP2Ce (iPP2Ce). PP2Ce expression was detected only from double transgenic hearts in the absence of tetracycline. PC is positive control from NRVM expressing adv-PP2Ce. **C.** Representative immunoblot analysis. **D.** Quantification of key proteins involving

in calcium homeostasis regulation in control and PP2Ce transgenic (TG) hearts. Number of replicates is labeled in each column as indicated. \*:  $p < 0.05$ , \*\*:  $p < 0.01$ . **E.** Calcium transient peak amplitudes ( $F/F_0$ ), time to peak and decay measured from isolated cardiomyocytes of control (n=8) and PP2Ce TG (n=8) hearts.

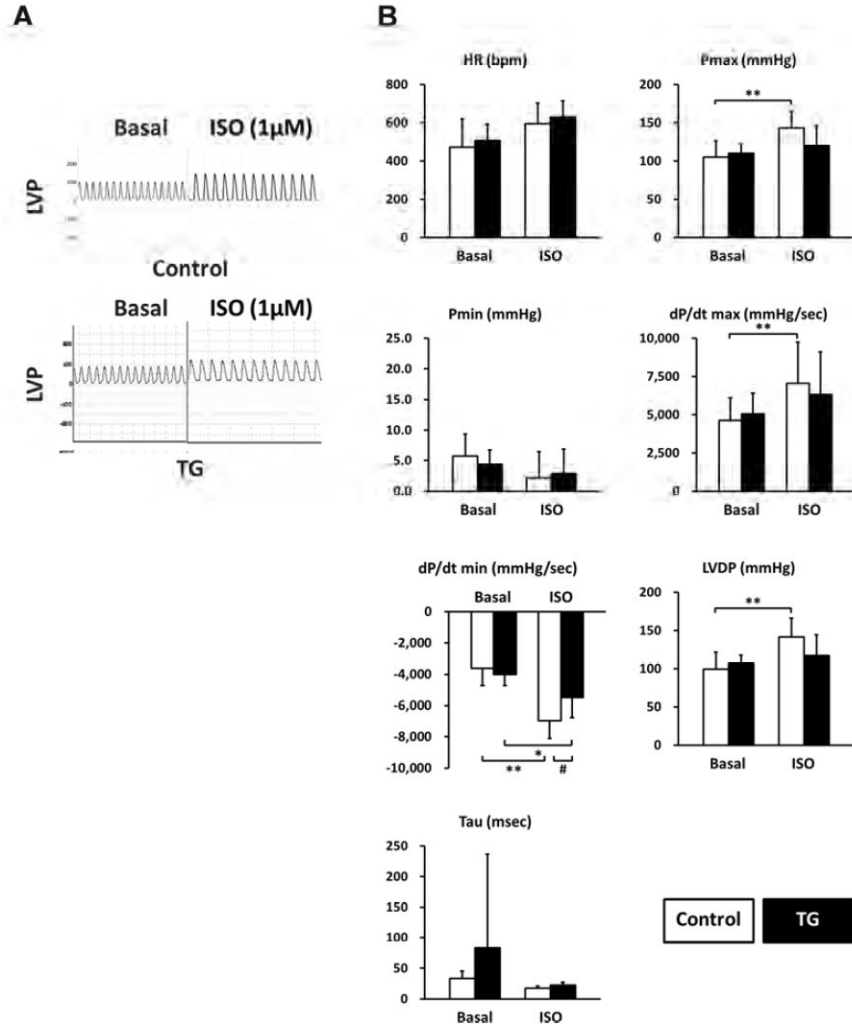
Author Manuscript

Author Manuscript

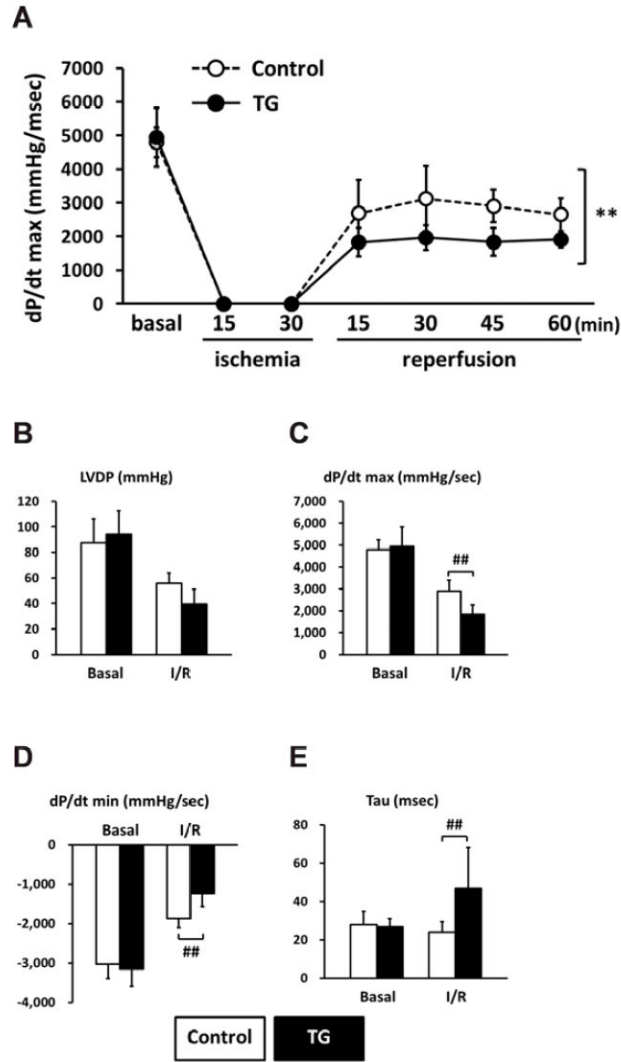
Author Manuscript

Author Manuscript

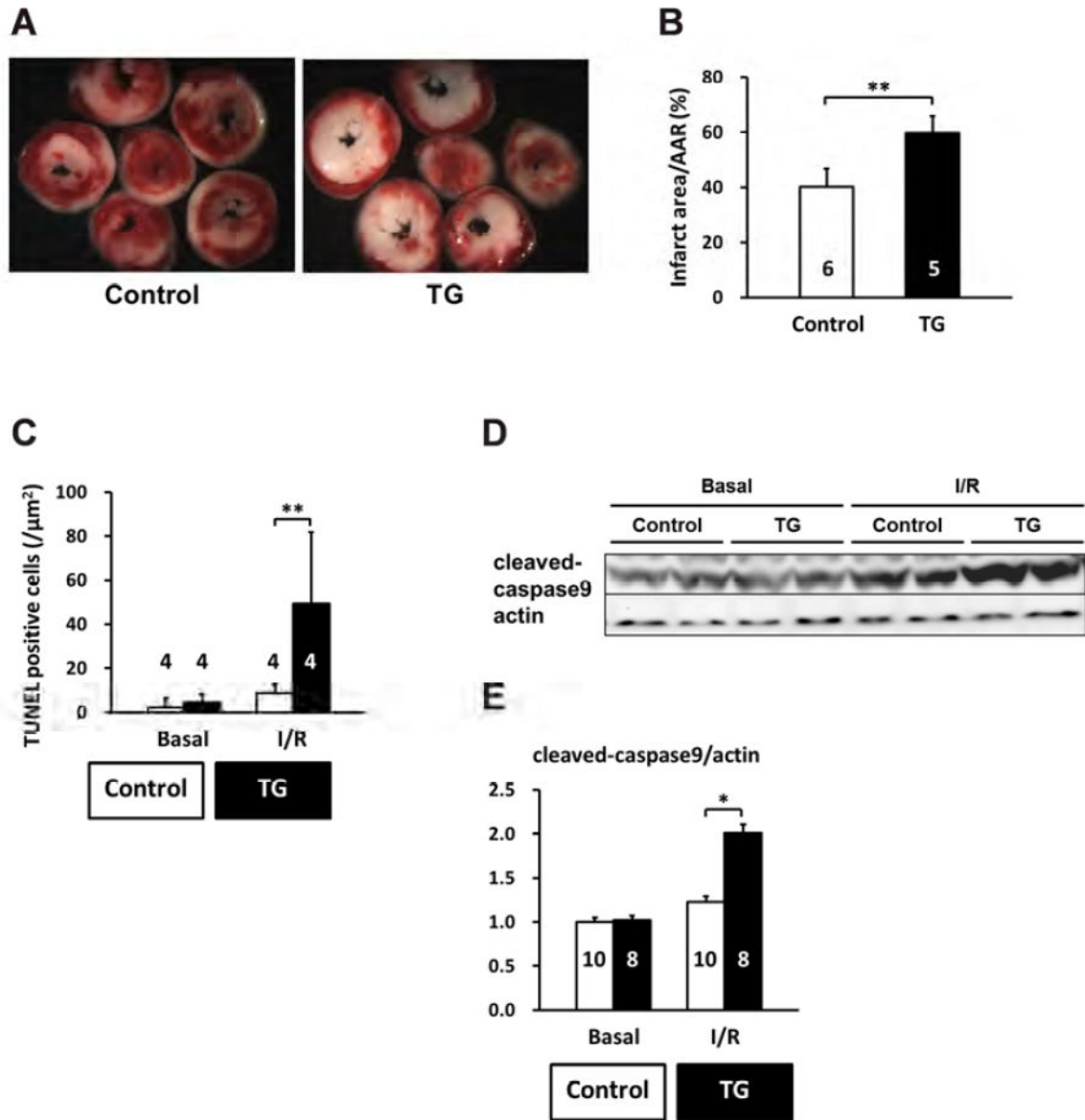




**Figure 8. PP2Ce expression impairs ISO stimulated enhancement of contractility**  
**A.** Representative left ventricle pressure (LVP) measured from isolated hearts of wildtype or PP2Ce TG mice at basal or perfused by 1µM of ISO. **B.** Hemodynamic parameters from control (n= 9) and PP2Ce TG (n=6) hearts at basal or treated by 10nM ISO. Pmax: maximal pressure, Pmin: minimal pressure, dP/dT: maximal or minimal pressure derivatives, LVDP: left ventricle developed pressure, Tau: relaxation index. \*:  $p < 0.05$ , \*\*:  $p < 0.01$  between basal and I/R within control or PP2Ce TG groups. #:  $p < 0.05$  between corresponding control and PP2Ce TG.

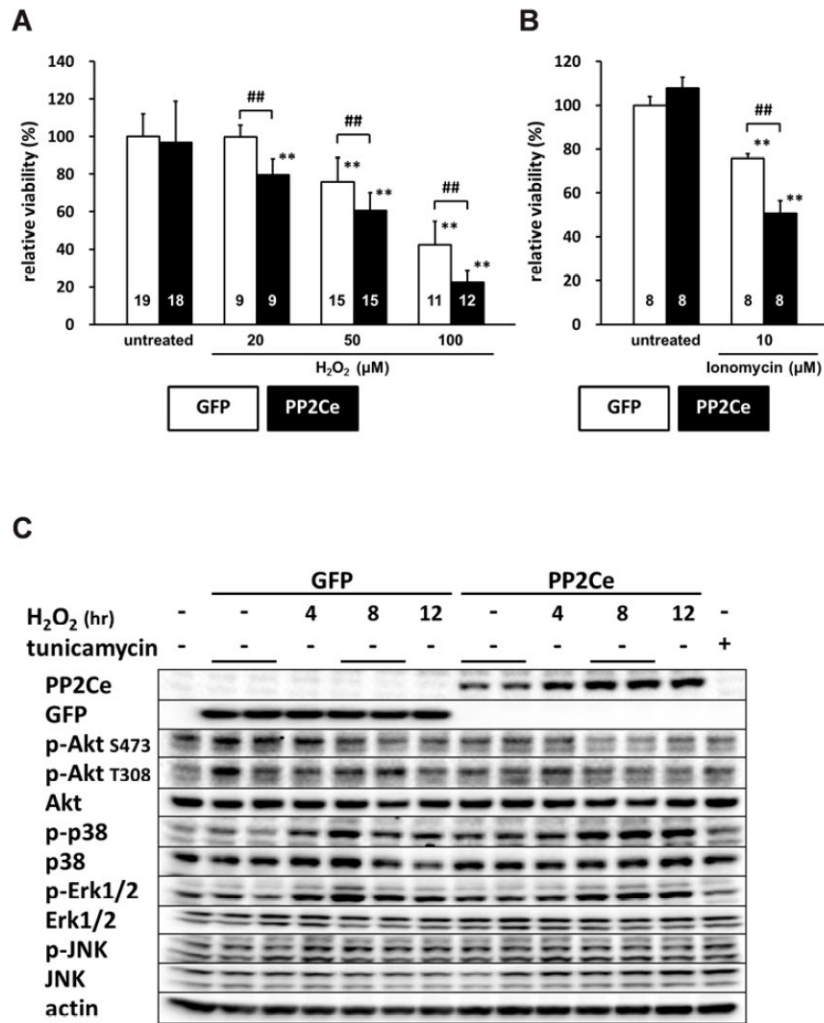


**Figure 9. PP2Ce expression impairs function recovery following ischemia/reperfusion injury**  
**A.** Left ventricle dP/dt max during 15 minutes global ischemia followed by 60 minutes reperfusion in isolated hearts from non-transgenic controls (Control, n=9) and PP2Ce TG (TG, n=6) mice. \*:  $p < 0.01$  between control and PP2Ce TG groups. Left ventricle function parameters measured as **(B)** left ventricular developed pressure (LVDP). **(C)** systolic pressure increase (dP/dt max) and **(D)** diastolic pressure decrease (dP/dt min) and **(E)** relax time index (tau) in non-transgenic controls (Control, n=9) and PP2Ce TG hearts (n=6) at basal and 45 minutes after reperfusion. #:  $p < 0.05$ , ##:  $p < 0.01$  between corresponding control and PP2Ce TG groups at each time points.



**Figure 10. Induced PP2Ce expression promotes cardiomyocyte death in response to ischemia/reperfusion injury**

**A.** Representative TTC staining cross-section images from one PP2Ce transgenic (TG) and one control (control) heart following 15 minutes of ischemia and 120 minutes of reperfusion (I/R). **B.** Infarct sizes of control (n=5) and PP2Ce transgenic (TG, n=6) hearts as measured from A. \*\*:  $p < 0.01$  between control and PP2Ce TG groups. **C.** Apoptotic index measured by TUNEL staining in control (n=4) and PP2Ce TG (n=4) hearts. \*\*:  $p < 0.01$  between corresponding control and PP2Ce TG groups. **D.** Representative immunoblot for level of activated caspase9 in control (n=10) and PP2Ce transgenic (TG, n=8) hearts following the same I/R protocol. **E.** Quantification of level of cleaved caspase9 signal from immunoblots. \*:  $p < 0.05$  between control and PP2Ce TG groups.



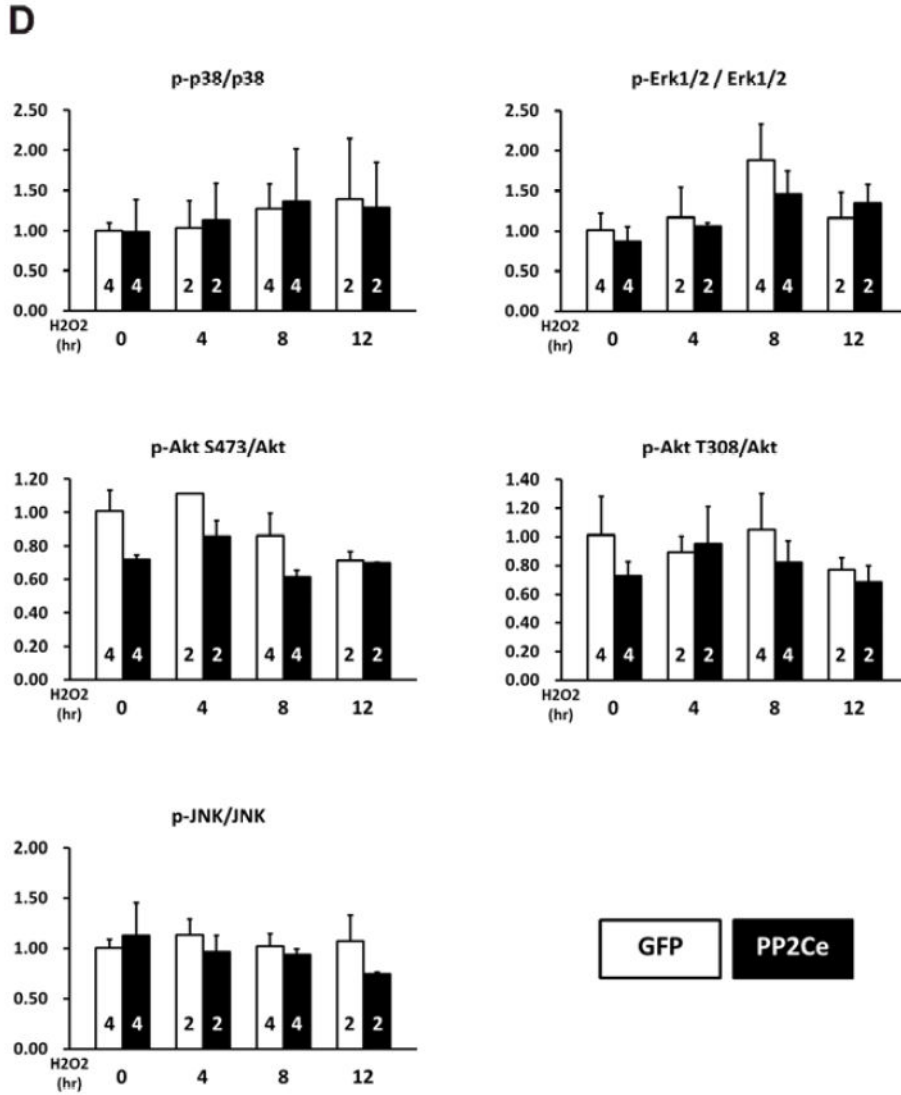


**Figure 11. PP2Ce expression promotes myocytes death and perturbs pro-survival signaling following oxidative injury**

**A.** NRVMr viability measured by MTT assay in NRVM expressing GFP or PP2Ce following H<sub>2</sub>O<sub>2</sub> treatment for 16 hours at different doses as indicated. Replicate number is labeled in each corresponding columns. \*\*:  $p < 0.01$  vs. untreated. ##:  $p < 0.01$  between GFP and PP2Ce groups at same doses. **B.** NRVM viability expressing GFP (n= 8) or PP2Ce (n=8) under untreated or following 24 hours of treatment of 2 $\mu$ M ionomycin. \*\*:  $p < 0.01$  vs. untreated. ##:  $p < 0.01$  between GFP and PP2Ce groups. **C.** Immunoblot analysis of intracellular signaling molecules as indicated in NRVM expressing GFP or PP2Ce with 50 $\mu$ M H<sub>2</sub>O<sub>2</sub> treatment at different time points as indicated. tunicamycin (5 $\mu$ g/ml for 4 hours) was used as a control. **D.** Quantification of signaling molecules as indicated with independent experimental replicate number labeled in each column.

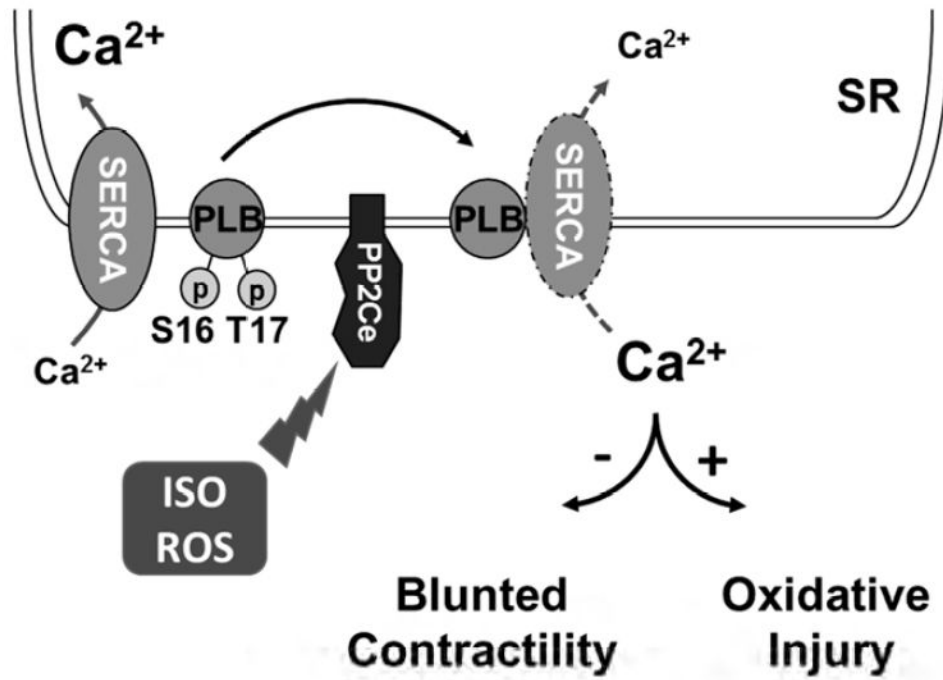


Figure 12. Illustration of PP2Ce function in cardiac myocytes

Echocardiogram parameters measured from non-transgenic (Control, n=41) and PP2Ce transgenic (TG, n=33) heart.

**Table 1**

	HR (bpm)	LVPW(s) (mm)	LVPW(d) (mm)	LVID(s) (mm)	LVID(d) (mm)	FS (%)
<b>Control (n=41)</b>	484±86	1.00±0.12	0.66±0.12	2.86±0.34	4.13±0.33	31.1±4.8
<b>TG (n=33)</b>	479±36	1.06±0.14 *	0.68±0.15	2.70±0.23 *	4.11±0.23	34.0±4.7 **

Values are mean ± SEM. HR: heart rate, FS: fractional shortening, LVPW: left ventricle posterior wall thickness (s) systolic or (d) diastolic, LVID: left ventricle internal dimension.

\*  $p < 0.05$ ,

\*\*  $p < 0.01$  between Control and TG groups.

**Table 2**

Hemodynamic parameters. Cardiac performance was measured from isolated non- transgenic (Control, n=9) and the PP2Ce transgenic (TG, n=6) hearts under basal (Basal) and post 30 mins global ischemia and 45 mins reperfusion (I/R).

	Control (n=9)		TG (n=6)	
	Basal	I/R	Basal	I/R
<b>HR (bpm)</b>	403.5±96.4	334.7±87.2	390.0±74.6	281.8±49.9
<b>Pmax (mmHg)</b>	91.22±20.67	95.50±10.60	98.55±17.72	94.35±10.42
<b>Pmin (mmHg)</b>	3.68±2.30	39.71±12.52##	4.28±2.44	55.03±11.26***
<b>dP/dt max (mmHg/sec)</b>	4794.9±446.4	2906.0±490.8##	4942.2±871.5	1839.8±411.0***
<b>dP/dt min (mmHg/sec)</b>	3031.6±359.8	1867.3±235.3##	3156.9±435.6	1225.6±344.6***
<b>LVDP (mmHg)</b>	87.54±18.76	55.79±8.31##	94.27±18.45	39.33±11.64 ##

Values are means ± SEM. HR: heart rate, Pmax: systolic pressure, Pmin: diastolic pressure, dP/dt max: maximal systolic pressure derivative, dP/dt min: maximal diastolic pressure derivative, LVDP: left ventricle developed pressure (Pmax-Pmin).

\*  $p < 0.05$ ,

\*\*  $p < 0.01$  between corresponding Control and TG groups.

##  $p < 0.01$  between basal and I/R within Control or TG groups.